Liquid Metal Bandwidth Reconfigurable Antenna

Khaled Yahya Alqurashi, James R. Kelly, *Member, IEEE,* Zhengpeng Wang, *Member, IEEE,* Carol Crean, Raj Mittra, *Life Fellow IEEE,* Mohsen Khalily, Senior *Member, IEEE* Yue Gao, *Senior Member, IEEE.*

***Abstract*— This paper shows how slugs of liquid metal can be used to connect/disconnect large areas of metalisation and achieve radiation performance not possible by using conventional switches. The proposed antenna can switch its operating bandwidth between ultra-wideband and narrowband by connecting/disconnecting the ground plane for the feedline from that of the radiator. This could be achieved by using conventional semiconductor switches. However, such switches provide point-like contacts. Consequently, there are gaps in electrical contact between the switches. Surface currents, flowing around these gaps, lead to significant back radiation. In this paper, slugs of liquid metal are used to completely fill the gaps. This significantly reduces the back radiation, increases the boresight gain, and produces a pattern identical to that of a conventional microstrip patch antenna. Specifically, the realised gain and total efficiency are increased by 2 dBi and 24%, respectively. The antenna has potential applications in wireless systems employing Cognitive Radio and Spectrum Aggregation.**

***Index Terms*— Bandwidth reconfiguration, Cognitive Radio, liquid metal, microstrip antenna, monopole antenna, reconfigurable antennas, Spectrum Aggregation, UWB antennas.**

I. Introduction and Motivation

TRADITIONALLY, semiconductor switches and varactors have been used to reconfigure antennas and the technology in this area is quite mature. However, it suffers from several limitations including: (i) significant overall power consumption; (ii) poor harmonic performance; and (iii) limited tuning range. Liquid metals, based on Gallium alloys, have the potential to address all of these issues. For these reasons interest in liquid metal, as a means of reconfiguring antennas, has grown over the last few years. The feasibilities of pattern-, frequency-, and polarisation-reconfigurable antennas have all been demonstrated in numerous recent publications [1-5]. However, to date, liquid metal has mostly been used to create relatively simple forms of reconfigurable antennas where the movement of liquid metal is used to alter the length of a wire or act as a switch. Although quite interesting, this type of functionality could also be achieved by using conventional semiconductor switches.

This paper shows how liquid metal can be used to completely bridge the full length of a gap between two large areas of metalisation, and obtain levels of radiation performance that would be impossible to achieve using conventional semiconductor switches. By altering the configuration of the ground plane, the antenna, presented herein, can switch its frequency operating bandwidth from ultra-wideband (UWB) to narrowband.

The proposed antenna has been designed to meet the requirements of Cognitive Radio (CR). Some experts suggest that CRs will require an UWB antenna to perform the sensing function. A narrowband antenna would then handle communications between the CR nodes. The UWB sensing antenna requires an omni-directional radiation pattern, in order to detect signals that may arrive from any direction. The narrowband antenna, used for communications, requires a directional radiation pattern because the node with which we wish to communicate is located at a known position. For applications having limited PCB real estate, the two antennas should be integrated into the same volume of space. The literature contains a number of designs for antennas that can be reconfigured between UWB/wideband and narrowband performance. However, most of those designs [6-12] provide an omni-directional radiation pattern within both modes of operation. The geometry of many of the designs is complex [7], [8], [11]. For this reason, as well as due to a lack of design rules, it would be both difficult and time-consuming to redesign those antennas to cover a different set of operating frequency bands. A number of the antennas rely on the use of an external filter which is integrated into the feedline [8-11]. Unfortunately, the use of an external filter increases the size of the antenna. Additionally, all of these antennas are reconfigured by using

Manuscript received April 8th 2019. We would like to acknowledge the support of the University of Surrey 5GIC (http://www.surrey.ac.uk/5gic) members for this work.

Khaled Yahya Alqurashi is with the Institute for Communication Systems (ICS), Department of Electrical and Electronic Engineering, University of Surrey, U.K. (e-mail: k.alqurashi@surrey.ac.uk).

Z. P. Wang is with the School of Electronics and Information Engineering, Beihang University, China (e-mail: wangzp@buaa.edu.cn).

Carol Crean is with the Department of Chemistry, University of Surrey, U.K. (e-mail: c.crean@surrey.ac.uk).

R. Mittra is with The Electromagnetic Communication Laboratory, University of Central Florida, Orlando, FL 32816 USA, and also with King Abdulaziz University, Jeddah 21589, Saudi Arabia (email: rajmittra@ieee.org).

M. Khalily is with the Institute for Communication Systems (ICS), Department of Electrical and Electronic Engineering, University of Surrey, U.K. (e-mail: m.khalily@surrey.ac.uk).

J. R. Kelly and Yue Gao are with the School of Electronic Engineering and Computer Science, Queen Mary University of London, UK. (e-mail: {j.kelly, yue.gao}@qmul.ac.uk).

conventional semiconductor switches and/or varactors, so they suffer from the limitations described above.

The paper is organised as follows. Section II explains the concept, design, and prototyping of the proposed antenna. Section III presents the simulation and measurement results. Finally, Section IV draws overall conclusions.

II. Antenna Concept, Design and Prototyping

A planar monopole antenna is similar in appearance to a microstrip patch antenna. The key difference is that, in a planar monopole antenna, there is no ground plane beneath the radiating element. In terms of performance, a monopole antenna yields a wide or ultra-wide operating frequency bandwidth. Whereas a microstrip patch antenna only radiates efficiently over a narrowband of frequencies. The realisation that such a dramatic difference in performance could be caused by such a simple change in geometry, led us to pose the question: What would happen if the ground plane, beneath the radiating element, could be switched ON and OFF? The antenna developed to address this question was reported in the literature [13, 14].

This paper presents an improved design using liquid metal. The proposed antenna, shown in Fig. 1, has an overall size of 30 mm by 38 mm. Both the original and proposed antennas incorporate three segments of ground plane (i.e., Ground #1 to Ground #3), as shown in Fig. 1(b).

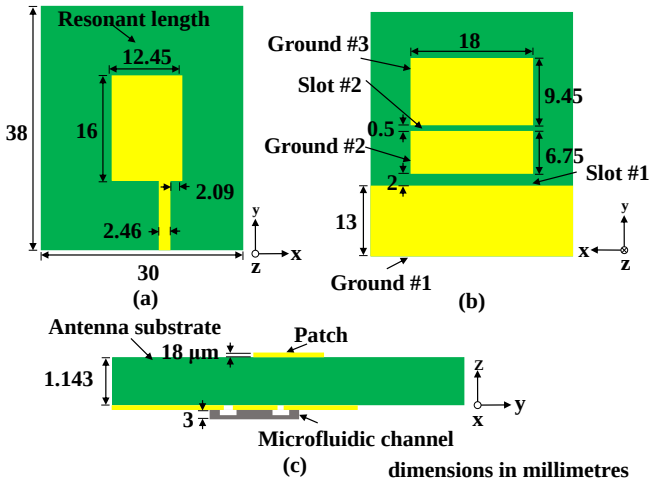

Fig. 1. Proposed antenna. (a) front view, (b) rear view, (c) side view.

In the proposed antenna, Slot #1 is used to isolate the ground plane for the microstrip line (Ground #1) from the ground plane for the radiator (Ground #2 and Ground #3). Slot #2 is used to remove a notch band from the performance of the antenna in the ultra-wideband (UWB) state. Three hardwired switches were used in the original antenna to connect the three ground planes. In the proposed antenna, those switches are replaced with two slugs of liquid metal which fill Slots #1 and #2. When both slugs of liquid metal are in place, the ground plane for the microstrip transmission line (Ground #1) is joined to the ground plane for the radiating element (Grounds #2 and #3). This causes the antenna to enter the narrowband operating state. When both slugs of liquid metal are removed, the ground plane for the microstrip line (Ground #1) is disconnected from the ground plane for the radiating element (Grounds #2 and #3), causing the antenna to enter the UWB operating state.

In the narrowband operating mode, the use of liquid metal within the proposed antenna offers the following advantages compared with the use of semiconductor switches: (i) reduced back radiation; (ii) 2 dB additional realised gain; (iii) conventional microstrip patch radiation pattern; (iv) improved S_{11} performance; (v) greatly reduced harmonic distortion. These advantages accrue from the way that liquid metal can completely bridge the slots in the ground plane in a way that would be impossible to achieve by using conventional switches. Furthermore, when using liquid metal, the gap sizes can be optimised without the constraint of switch dimensions.

Fig. 2 shows a hardware prototype that is fabricated and measured for validation purposes. The copper parts of the antenna are fabricated on a 1.143 mm-thick Taconic TLY-5 substrate (ε_r = 2.2, tan δ = 0.0009 at 10 GHz).

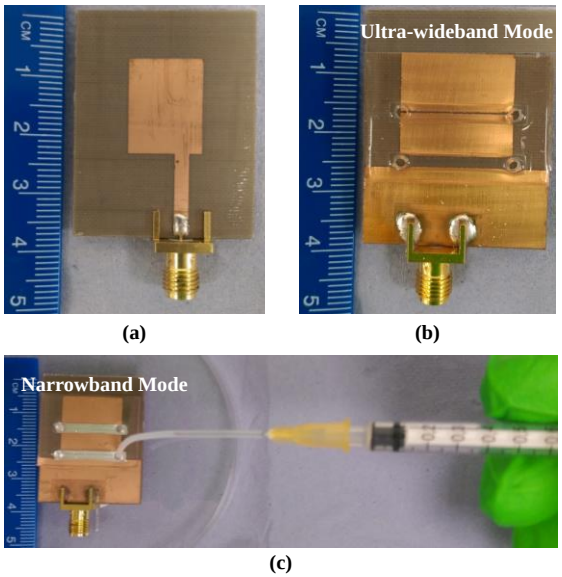

Fig. 2. Fabricated antenna prototype. (a) front view, (b) rear view – UWB mode, (c) rear view – narrowband mode (i.e. Slots #1 and #2 filled).

The two slugs of liquid metal are contained within microfluidic channels formed from Polydimethylsiloxane (PDMS) sold under the tradename SYLGARD(R) 184 silicone elastomer (ε_r = 2.67, tan δ = 0.02 at 3 GHz). Each channel is 2.5 mm wide and 1 mm high. The entire PDMS structure is 21 mm x 30 mm x 3 mm. Two inlet/outlet holes are incorporated within each channel to facilitate actuation (i.e., insertion/removal) of liquid metal. In this antenna, the slugs of liquid metal make direct contact with the copper ground planes. A commercially available liquid metal alloy, known as EGaIn, is employed.

The liquid metal is injected/removed by using a syringe, as shown in Fig. 2(c). This is a commonly used approach described in the literature. Alternative methods of actuation have been reported in the literature, including: electrochemically controlled capillary action and the use of a micropump, and one of these existing techniques could be employed in this application. However, liquid metal actuation is not the main focus of the paper. Moreover, altering the method of actuation would have minimal effect on the RF performance of the proposed antenna because the microfluidic structure is located beneath the ground plane where the electric and magnetic field strength is low.

A video of the channel being filled was captured. The approximate filling time, determined from the video, was three seconds. This therefore represents the time required to manually switch between the narrowband and UWB state of operation. The reconfiguration time could be significantly shortened by connecting all of the inlets/outlets in parallel to a bidirectional micropump (e.g. mp5, Bartels Mikrotechnik GmbH).

III. Results and Analysis

This section presents simulation and measurement results for the antenna. The full-wave simulation results were obtained by using the Transient Solver in CST Microwave Studio® 2018.

The reflection coefficient curves pertaining to the narrow and UWB operating states are shown in Fig. 3. The antenna performs well in both operating states, and there is good agreement between the measurement and simulation results.

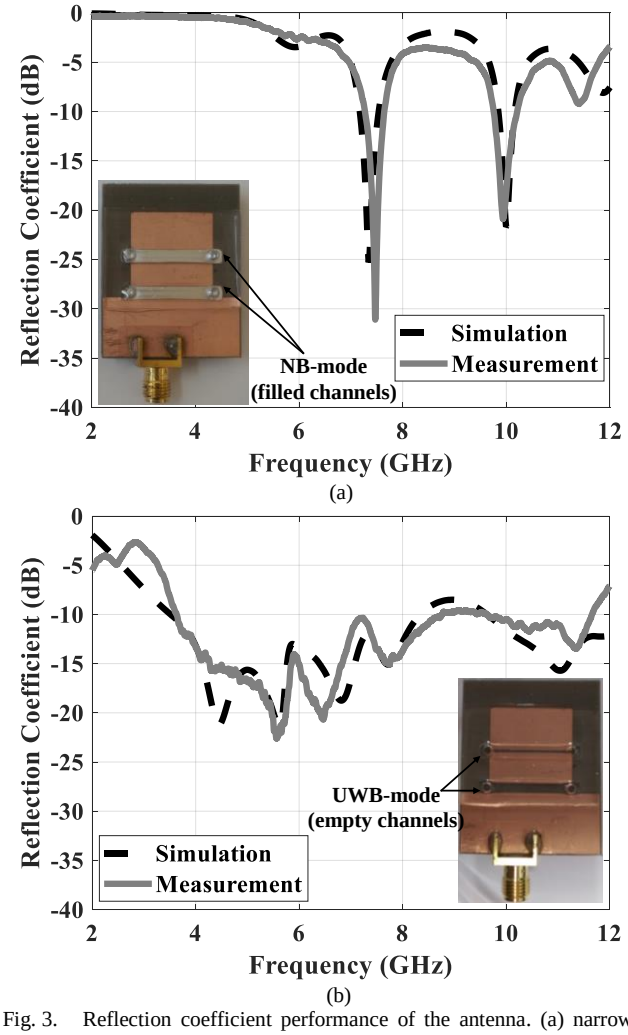

Fig. 3. Reflection coefficient performance of the antenna. (a) narrowband (NB) operating state, (b) ultra-wideband (UWB) operating state.

Both slugs of liquid metal must be in place to achieve the narrowband mode of operation, as explained earlier. The deepest resonance in Fig. 3(a) is that associated with the TM_{10} mode (denoted f_{10}). This is the fundamental mode associated with a conventional rectangular microstrip patch antenna. Specifically, it is located at the frequency for which the resonant length of the radiating patch (marked in Fig. 1) corresponds to one-half of the guided-wavelength. In the reflection coefficient curves, obtained through measurement and simulation, f_{10} is located at 7.47 GHz and 7.34 GHz, respectively. When both slugs of liquid metal are removed the antenna enters the UWB operating state. It is evident from the measured results, shown in Fig. 3(b) that the curve remains below the commonly applied -10 dB reflection coefficient threshold from 3.63 GHz to 8.76 GHz. The measured reflection coefficient curve remains below -9.6 dB from 3.59 GHz to 11.69 GHz. The curve attains its peak value of -9.6 dB at a frequency of 9.10 GHz. It is not possible to fully remove this notch, owing to the trade-off between the design choices required to realise good performance in the narrowband operating state and those that simultaneously provide good performance in the UWB operating state. Nonetheless, the -10 dB S_{11} bandwidth of the antenna, realised by the compromise choice, covers the UWB in the U.K. (i.e. 3.1 - 4.8 GHz and 6.0 - 9.0 GHz) [15].

The original antenna [13, 14] incorporated three hardwired switches. Unfortunately, the switches only provide contact between narrow (point-like) areas of metalisation. Consequently, there are gaps in electrical contact between the switches. In the narrowband mode, a strong standing wave distribution of surface current exists around these gaps in the ground plane. By contrast, the current on the patch is low.

Fig. 4 plots the 3D radiation patterns (realised gains) associated with the original and proposed antennas. Fig. 4(b) shows that the strong currents around the slots in the ground plane, of the original antenna, lead to high levels of back radiation, i.e. along the *z*-axis direction. This distorts the radiation pattern and, as a result, it no longer resembles that of a conventional microstrip patch antenna. The situation could be improved by employing a large number of switches connected in parallel. However, that would increase the RF power dissipation (thus reducing gain) as well as the DC power required for biasing. To address this problem, we use slugs of liquid metal to bridge (and thus completely eliminate) the gaps

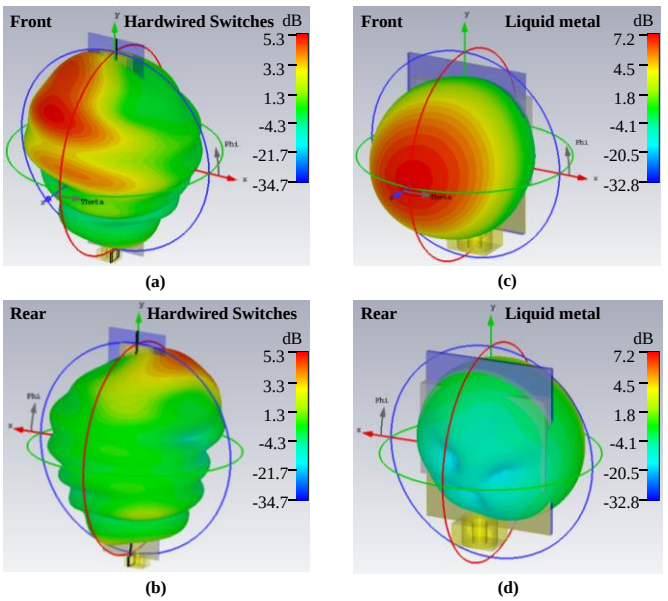

Fig. 4. 3D radiation patterns (realised gains). (a) and (b) front and rear views of original (hardwired switches) antenna [13, 14]; (c) and (d) front and rear views of proposed antenna incorporating slugs of liquid metal.

in the ground plane. Inspection of Fig. 4(d) reveals that this greatly reduces the level of back radiation. Fig. 5 shows the polar radiation patterns for the proposed antenna in the narrowband operating state at the frequency of the fundamental mode. The radiation patterns associated with the proposed antenna are essentially those of a conventional patch antenna, see Figs. 4(c), 4(d), and 5. According to the simulations, the antenna has a realised gain of 7.2 dBi and a total efficiency of 95% at the narrowband resonant frequency of 7.34 GHz. The measured resonant frequency of the fabricated prototype was 7.47 GHz. The realise gain was measured, at this frequency, using the 2 antenna method. The measured co- and cross-polar gain values are: 7.0 dBi and -4.57 dBi, respectively.

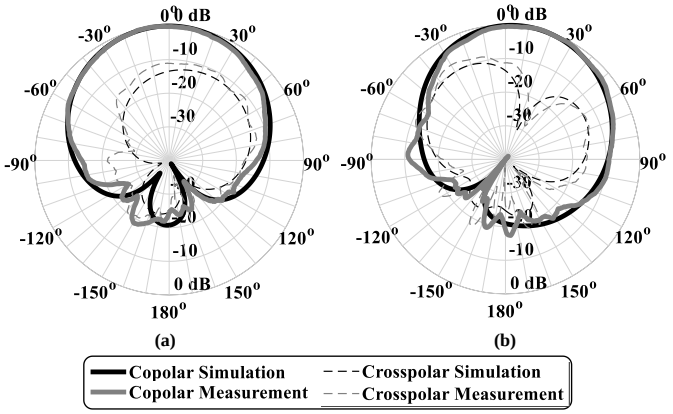

Fig. 5. Polar radiation patterns for proposed antenna in narrowband operating state of fundamental mode. (a) *xz*-plane, (b) *yz*-plane.

Computer simulations were performed to compare the effect of using liquid metal to that of using solid copper or PIN diodes in the narrowband mode. Table I summarises the results.

The first row of Table I presents the performance of the antenna when Slots #1 and #2 are filled with copper. The radiation performance, second row, remains virtually unchanged when the slots are filled with slugs of liquid metal instead. The reason for this is that the conductivity of liquid metal (σ = 3.6 x 10^6 S/m) is only around one order of magnitude lower than that of copper (σ = 5.8 x 10^7 S/m). The third row of Table I shows the effect of removing the microfluidic channel structure. The dielectric loss of the PDMS has a negligible effect, since it is located beneath the ground plane where both the electric and magnetic field strengths are low. Finally, in the fourth row, the effect of using PIN diodes (BAR50-02V, Infineon Technologies) is examined. The diode is modeled by using an equivalent circuit and inserted across the three switch locations proposed by [13, 14].

Table I
Narrowband Mode: Radiation Performance Comparison.

Material/Technique	Frequency (GHz)	Realised Gain (dBi)	Radiation Efficiency (%)
Copper	7.34	7.2	96
Liquid Metal	7.34	7.2	96
Liquid Metal where PDMS removed	7.33	7.3	96
Diode	7.66	5.1	72

The simulations reveal that, in comparison with liquid metal, the use of PIN diodes shifts the resonant frequency and reduces the radiation efficiency by 24%. Both of these effects are undesirable and are alleviated by using liquid metal. Moreover, a total of 10 hardwired (ideal) switches or 18 PIN diode switches would be required to realise a level of performance similar to that which we would obtain by using liquid metal.

Fig. 6 presents the polar radiation patterns of the antenna in the UWB operating state. The *xz*-plane patterns are approximately omni-directional, whereas the *yz*-plane patterns are shaped like a figure-of-eight, as expected for a monopole. The antenna attains a maximum simulated realised gain of 5.6 dBi at 7.33 GHz. The minimum values of simulated total efficiency and realised gain are 92% and 2.4 dBi, respectively, at 4.05 GHz and 7.74 GHz.

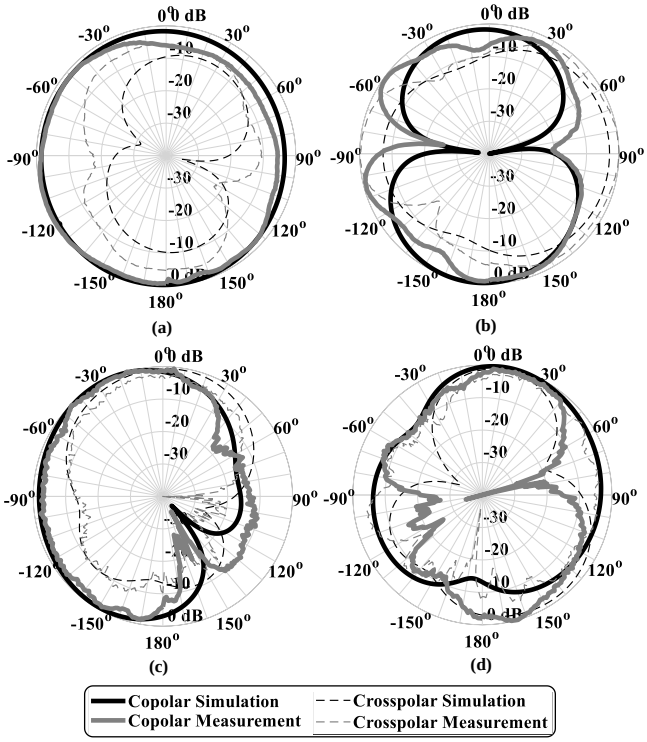

Fig. 6. Polar radiation patterns for UWB state. (a), (c) *xz*-plane at 4.05 GHz and 7.74 GHz. (b), (d) *yz*-plane at 4.05 GHz and 7.74 GHz.

IV. Conclusions

The antenna reported in this paper is reconfigured by altering the apparent location of its ground plane with respect to the radiating element. The reconfiguration required to make this work effectively, without performance degradation, would simply be impossible to realise, by using conventional semiconductor switching and tuning technologies. The antenna is capable of switching its operating frequency bandwidth between UWB and narrowband. The measured narrowband state resonates at 7.47 GHz with a simulated realised gain of 7.2 dBi and a measured gain of 7.0 dBi. The measured S_{11} bandwidth in the UWB-state ranges from 3.59 GHz to 11.69 GHz ($S_{11} \leqslant$ -9.6 dB) with a maximum simulated realised gain of 5.6 dBi at 7.33 GHz. This antenna will be of value in applications requiring bandwidth switching, e.g. Cognitive Radio and Spectrum Aggregation.

REFERENCES

[1] D. Rodrigo, L. Jofre, B.A. Cetiner, "Circular Beam-Steering Reconfigurable Antenna With Liquid Metal Parasitics," IEEE Trans. Ant. Propag., 2012, vol. 60, no. 4, pp. 1796-1802

[2] A. Gheethan, R. Guldiken, G. Mumcu, "Microfluidic enabled beam scanning focal plane arrays," IEEE Antennas and Propagation Society International Symposium (APSURSI), 2013, pp. 208 - 209

[3] A.P. Saghati, J.S. Batra, J. Kameoka, K. Entesari, "A Microfluidically Reconfigurable Dual-Band Slot Antenna With a Frequency Coverage Ratio of 3:1," IEEE Ant. Wireless Propag. Lett., vol. 15, pp. 122-5, 2016.

[4] S.J. Mazlouman, X.J. Jiang, A.N. Mahanfar, C. Menon, et al "A Reconfigurable Patch Antenna Using Liquid Metal Embedded in a Silicone Substrate," IEEE Trans. Ant. Propag., vol 59, pp. 4406-12, 2011.

[5] C. Wang, J.C. Yeo, H. Chu, C.T. Lim, et al. "Design of a Reconfigurable Patch Antenna Using the Movement of Liquid Metal," IEEE Ant. and Wireless Propag. Lett., vol. 17, no. 6, pp. 974-77, 2018.

[6] Cristina Borda-Fortuny, Kin-Fai Tong, Kevin Chetty, "Low-cost mechanism to reconfigure the operating frequency band of a Vivaldi antenna for cognitive radio and spectrum monitoring applications," IET Microwaves, Antennas & Propagation, vol. 12, no. 5, 2018.

[7] Gunjan Srivastava, Akhilesh Mohan, Ajay Chakrabarty, "Compact Reconfigurable UWB Slot Antenna for Cognitive Radio Applications," IEEE Antennas and Wireless Propagation Letters, vol. 16, 2017.

[8] Ali Mansoul, Farid Ghanem, Mohamad R. Hamid, Erkki Salonen, Markus Berg, "Bandwidth reconfigurable antenna with a fixed lower and a variable upper limit," IET Microwaves, Antennas & Propagation, vol. 10, no. 15, 2016.

[9] Pei-Yuan Qin, Feng Wei, Y. Jay Guo, "A Wideband-to-Narrowband Tunable Antenna Using A Reconfigurable Filter," IEEE Transactions on Antennas and Propagation, vol. 63, no. 5, 2015.

[10] Bei-Jia Liu, Jing-Hui Qiu, Sheng-Chang Lan, Guo-Qiang Li, "A Wideband-to-Narrowband Rectangular Dielectric Resonator Antenna Integrated With Tunable Bandpass Filter," IEEE Access, vol. 7, 2019.

[11] Saffrine Kingsly, Deepa Thangarasu, Malathi Kanagasabai, Mohammed Gulam Nabi Alsath, et al., "Multiband Reconfigurable Filtering Monopole Antenna for Cognitive Radio Applications," IEEE Antennas and Wireless Propagation Letters, vol. 17, no. 8, 2018.

[12] Xingxing Jiao, Junhong Wang, Ziwei Ying, "A Compact Two-Port Integrated UWB and Frequency Reconfigurable Antenna System for Cognitive Radio Application," 2019 IEEE MTT-S International Wireless Symposium (IWS), 2019.

[13] J.R. Kelly, E. Ebrahimi, P.S. Hall, P. Gardner, et al "Combined Wideband and Narrowband Antennas for Cognitive Radio Applications", in IET Seminar on Cognitive Radio and Software Defined Radio: Technologies and Techniques, London, UK, 2008.

[14] J.R. Kelly, and P.S. Hall, "Integrated Wide-Narrow Band Antenna for Switched Operation," Microw. and Optical Tech. Lett., vol. 52, no. 8, pp. 1705–7, Aug. 2010.

[15] ETSI EN 302 065: " Electromagnetic compatibility and Radio spectrum Matters (ERM); Short Range Devices (SRD) using Ultra Wide Band technology (UWB) for communications purposes; Harmonized EN covering the essential requirements of article 3.2 of the R&TTE Directive".